THE ASTROPHYSICAL JOURNAL, 298: 859–866, 1985 November 15

STUDIES OF HOT B SUBDWARFS. II. ENERGY DISTRIBUTIONS OF THREE BRIGHT sdB/sdOB STARS IN THE 950–5500 Å RANGE

F. WESEMAEL,[1,2,3] J. B. HOLBERG,[2,4] S. VEILLEUX,[3] R. LAMONTAGNE,[3] AND G. FONTAINE[1,2,3]
Received 1985 February 11; accepted 1985 May 20

ABSTRACT

Voyager ultraviolet spectrometer observations of the subdwarf B or OB stars HD 205805, UV 1758+36, and Feige 66 are presented. All three objects display the H I Lyman series in absorption. These observations are combined with low-dispersion *IUE* spectrophotometry and with Strömgren photometry to construct virtually complete energy distributions, which extend over the range 950–5500 Å. Effective temperatures based on model atmosphere calculations for high-gravity, hydrogen-rich stars are determined. Our analyses yield T_e = 28,200 ± 1300 K for HD 205805, T_e = 31,800 ± 1100 K for UV 1758+36, and T_e = 35,700 ± 1500 K for Feige 66. The importance of far-ultraviolet observations below Lyα in reducing the uncertainties associated with the interstellar extinction and the degradation of the *IUE* sensitivity is emphasized.

Subject headings: spectrophotometry — stars: atmospheres — stars: early-type — stars: subdwarfs — ultraviolet: spectra

I. INTRODUCTION

Recent investigations of the atmospheric properties of subluminous B stars (e.g., Heber *et al.* 1984*b*; Heber and Hunger 1984; Heber 1985) have been instrumental in improving our limited understanding of this much-neglected class of evolved, low-mass stars. Indeed, detailed atmospheric studies are necessary to understand not only the evolutionary status but also the importance of various physical processes likely to occur in the envelopes of these objects.

Because the subdwarf B stars all have $T_e \geq 20{,}000$ K, observations in the ultraviolet, near the peak of the energy distribution, provide additional help in determining the effective temperature. Such observations are possible, to some extent, with the use of the *IUE* longward of the Lyα line and have been shown to be useful for studies of hot B subdwarfs (Heber *et al.* 1984*b*; Heber and Hunger 1984; Heber 1985), despite uncertainties in the photometric accuracy of the instrument and, to a lesser extent, in the nature and amount of interstellar reddening along the line of sight. Recently, however, the region below ~1200 Å has also become accessible through the ultraviolet spectrometers on board the *Voyager 1* and *2* spacecraft (Broadfoot *et al.* 1977, 1981). Observations in the 911–1200 Å band from *Voyager* have already proved important for the detailed study of selected hot DA white dwarfs (e.g., Holberg *et al.* 1980; Holberg, Wesemael, and Hubený 1984; Holberg *et al.* 1985) and hot O subdwarfs (Drilling, Holberg, and Schönberner 1984); they have now been extended to a handful of bright B subdwarfs. These observations allow the construction of virtually complete energy distributions (911–5500 Å) which combine ultraviolet and optical observations and can be analyzed with stellar model atmosphere techniques.

The rationale for the study of combined optical, *IUE*, and *Voyager* energy distributions of hot B subdwarfs is thus twofold: First, such investigations permit us to extend significantly the wavelength baseline over which effective temperature determinations are performed, with, presumably, a corresponding increase in accuracy. Second, they help provide a check on the extent to which the current generation of model atmosphere calculations for these stars is able to reproduce the observations.

In the present paper, we analyze combined energy distributions for three subdwarf stars, selected on the basis of their intrinsic brightness. HD 205805 (FB 178, CZ 19489) and UV 1758+36 are two classical sdB stars. The first one, initially noticed by Newell (Sargent and Searle 1968), was analyzed by Baschek and Norris (1970). They determined $T_e = 26{,}500^{+1500}_{-1300}$ K from optical colors and hydrogen line profiles. The latter was discovered in the S2/68 Ultraviolet Sky Survey aboard the *TD-1* satellite (Boksenberg *et al.* 1973) and has been further observed in the optical by Giddings and Dworetsky (1978). These authors derive T_e = 32,500 ± 2500 K from hydrogen line profile fitting. The last object, Feige 66 (BD +25°2534, Malmquist 229, FB 103) is an OB subdwarf. Its spectrum shows, in addition to the hydrogen Balmer series, He I, He II, and S III lines (Berger 1963; Greenstein and Sargent 1974). The most recent study of this object is the differential analysis of Baschek, Höfflich, and Scholz (1982), who derive T_e = 36,000 ± 2200 K, on the basis of metal ionization equilibrium arguments.

In § II of this paper, we present the *Voyager*, *IUE*, and Strömgren observations used in the fits. The theoretical model energy distributions used in the fitting procedure are presented in § III, together with a brief discussion of our method. Results of this analysis are shown in § IV, where we also discuss the various uncertainties due to the *IUE* absolute calibration.

II. OBSERVATIONAL MATERIAL

a) The Voyager Observations

The ultraviolet spectrometers on the *Voyager 1* and *2* spacecraft are nearly identical objective grating spectrometers which

[1] Visiting Astronomer, Kitt Peak National Observatory, National Optical Astronomy Observatories, which is operated by the Association of Universities for Research in Astronomy, Inc., under contract with the National Science Foundation.

[2] Guest Investigator with the *International Ultraviolet Explorer* satellite, which is sponsored and operated by the National Aeronautics and Space Administration, by the Science Research Council of the United Kingdom, and by the European Space Agency.

[3] Département de Physique and Observatoire du mont Mégantic, Université de Montréal.

[4] Lunar and Planetary Laboratory, University of Arizona.

TABLE 1

Voyager OBSERVATION LOG

Object	*Voyager*	Date (year/day)	Integration (s)
HD 205805	*V1*	1982/108.3	6480
UV 1758+36	*V2*	1983/290.9	1509
Feige 66	*V2*	1982/210.5	4297

record the 500–1700 Å spectral range on an array of 126 photon counting detectors. A complete description of these instruments is given by Broadfoot *et al.* (1977), and a summary of their inflight performance is contained in Broadfoot *et al.* (1981). For a stellar source the spectral resolution is approximately 25 Å. The field of view on both instruments is 0°.1 (FWHM) in the dispersion direction by 0°.87 (FW) in the cross-dispersion direction. The location of a star within the field of view is determined through the use of spacecraft attitude-control error signals.

In Table 1 we provide a summary of spacecraft, date of observation, and effective integration time for our three targets. The effective integration time refers to the total duration of all on-axis spectra from which our fluxes are derived. Due to spacecraft limit cycle motions, this is generally a small fraction (5%–10%) of the total time devoted to the target. The observations described here were performed and reduced in a manner very similar to that described by Drilling, Holberg, and Schönberner (1984). Following sky background subtraction and removal of channel-to-channel variations and instrumental scattering, the resulting count rate spectra were placed on an absolute scale using the calibration of Holberg *et al.* (1982). In our subsequent analysis we employ fluxes derived from both *Voyager 1* and *2*. Both instruments have well-established mutual cross calibrations and identical dispersions of 9.26 Å per channel, so that our results can be considered independent of spacecraft. The only differences are a 21 Å displacement between the wavelength scales of the two instruments and a higher sensitivity for *Voyager 2*. Although *Voyager* spectra are recorded over the entire 1170 Å range of the detector, we only consider here the 912–1150 Å range. This is because, in the extreme ultraviolet, our target stars do not show any observable flux shortward of the Lyman limit. In addition, scattering from the intense interplanetary H I Lyα line and low detector sensitivity combine to reduce substantially the signal-to-noise ratio in the spectra at wavelengths longward of 1150 Å.

The resulting *Voyager* count rate spectra in the 900–1200 Å range are displayed in Figure 1. All three are characterized by a broad maximum near 1100 Å, together with a sharp decrease toward the Lyman edge. The first members of the hydrogen Lyman series are also detectable in absorption in all three objects. The region surrounding the Lyα λ1215 feature is dominated by the statistical uncertainty arising from the subtraction of the interplanetary Lyα emission feature.

b) *The IUE Observations*

Ultraviolet observations of our three targets were also obtained with the *International Ultraviolet Explorer* (*IUE*) satellite in the low-resolution mode. All observations were obtained through the large aperture and cover the region between 1150 and 3200 Å. Further details of these observations are presented in Table 2.

Both images of HD 205805 were processed with the standard *IUE* calibration procedure available at the Goddard Space Flight Center, as were the SWP image of Feige 66 and the LWR image of UV 1758+36. The SWP spectrum of the

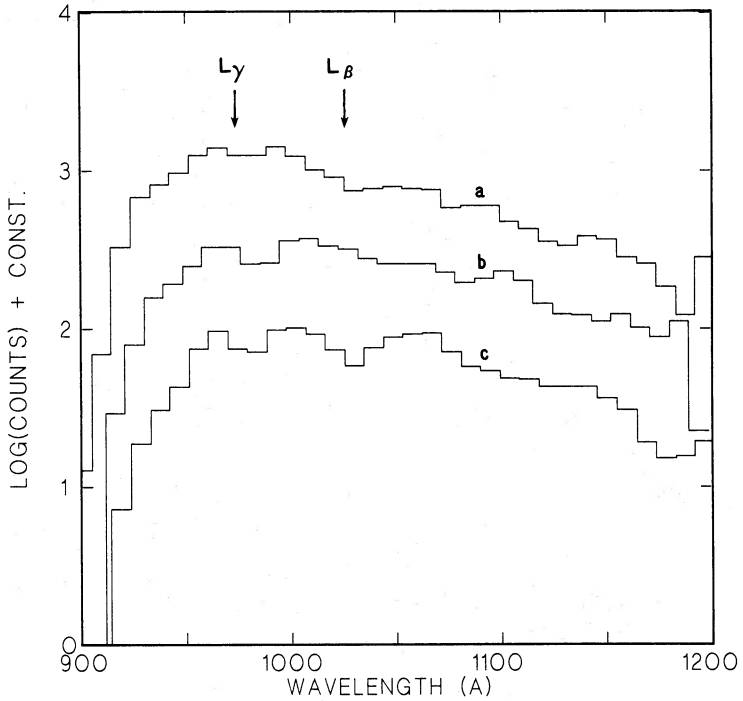

FIG. 1.—The *Voyager* 900–1200 Å count rate spectra for (*a*) Feige 66, (*b*) UV 1758+36, and (*c*) HD 205805. Absorption features due to H I Lyβ (λ1025) and Lyγ (λ972) are indicated. The Lyα (λ1215) region is overwhelmed by the large Lyα foreground correction.

TABLE 2

IUE OBSERVATION LOG

Target	Image	t_{exp} (s)	Source
HD 205805	SWP 20339	60	...
	LWR 16262	135	...
UV 1758+36	SWP 8078	155	Darius
	LWR 16578[a]	180	...
Feige 66	SWP 24551	62	...
	LWR 3016	272	Oke

[a] Image obtained in the course of a separate collaborative effort with E. M. Sion.

latter object was obtained from ESA through the National Space Science Data Center archives, which also provided the LWR spectrum of Feige 66, acquired at Goddard.

In addition to the standard reduction procedures, we have also considered additional correction algorithms for *IUE* data which have been discussed in the literature. The first one, described by Hackney, Hackney, and Kondo (1982), corrects for exposure-dependent continuum distortions in the SWP camera; these can cause flux deficits of up to 10% near 1650 Å. The Hackney *et al.* correction is included in all our analyses. A more serious concern about the reliability of *IUE*-based effective temperature determinations arises with the recent work of Finley, Basri, and Bowyer (1984, hereafter FBB). These authors discuss the wavelength-dependent sensitivity degradation of the *IUE* cameras over a ~3 yr period, and suggest that revisions in the overall *IUE* calibration of ~10% should be applied. While it may be premature to incorporate the FBB correction into our standard analysis, it is clearly interesting to explore its influence on the effective temperatures determined in the course of our investigation. Furthermore, as emphasized by FBB, the wavelength dependence of that correction is such that it has a pronounced peak at ~2200 Å, on top of the reddening hump. We have, accordingly, studied the importance of the FBB correction in our analysis, and this is discussed in detail in § IV*b*.

c) *The Strömgren Observations*

Narrow-band Strömgren magnitudes were used to complete the energy distributions of our three target stars, and these data are summarized in Table 3. The colors of HD 205805 were taken from Newell and Graham (1976); those of Feige 66 and UV 1758+36 were obtained within the course of our own investigation of the photometric properties of B subdwarfs (Bergeron *et al.* 1984; Fontaine *et al.* 1985). Feige 66 has also been observed by Graham (1970), and his colors are in good agreement with those of Bergeron *et al.* (1984). For the sake of consistency, we have used the latter values throughout our analysis. The Strömgren magnitudes were converted to absolute fluxes with the calibration of Heber *et al.* (1984*b*). Accordingly, a magnitude $m_\lambda = 0.000$ corresponds to absolute fluxes of 11.46×10^{-9}, 5.65×10^{-9}, and 3.60×10^{-9} ergs cm^{-2} s^{-1} Å^{-1} at *u*, *b*, and *y* respectively. The *v* magnitude was omitted from our analysis, as it is strongly affected by the Hδ line.

TABLE 3

SUMMARY OF STRÖMGREN PHOTOMETRY

Target	*y*	$(b-y)$	$(u-b)$	Source
HD 205805	10.21	−0.114	−0.032	1
UV 1758+36	11.37	−0.131	−0.188	2
Feige 66	10.56	−0.141	−0.227	3

SOURCES.—(1) Newell and Graham 1976. (2) Fontaine *et al.* 1985. (3) Bergeron *et al.* 1984.

For all three objects, we have adopted the following average rms errors for the photometric data: $\sigma_y = 0.03$, $\sigma_{b-y} = 0.018$, $\sigma_{u-b} = 0.044$. These represent the average rms differences between the Strömgren colors of Bergeron *et al.* (1984) and those of Graham (1970) or Graham and Slettebak (1973) for a sample of 14 B subdwarfs common to both investigations. The associated error bars are displayed in Figures 2–4.

III. TOOLS AND PROCEDURE

a) *The Models*

We have used two basic sets of model atmosphere calculations to analyze these observations. The first set consists of a series of metal-free hydrogen-line blanketed LTE models of hydrogen-rich composition (He/H = 10^{-2}) at log g = 5.0 and 6.0. The grid extends from T_e = 20,000 K to 56,000 K. The adopted gravities bracket those generally determined for B and OB subdwarfs (e.g., Heber *et al.* 1984*b*). Small gravity variations affect only the Lyman line region, but not the Balmer continuum slope. The chosen helium-to-hydrogen ratio is also typical of the helium-deficient B subdwarfs. Once again, however, small variations within the range characterizing the sdB stars would have no impact on the effective temperatures determined here. The input physics used in the calculation of these models is similar to that described in Wesemael *et al.* (1980). For these models, detailed energy distributions in the 911–5500 Å range were calculated to fit the observations. For the hydrogen lines the broadening theories of Vidal, Cooper, and Smith (1973) and Edmonds, Schlüter, and Wells (1967) were used. Discrete transitions up to 1–7 (λ931) were taken into account, as the treatment of the higher Lyman lines is important for a detailed fit to *Voyager* data on hydrogen-rich stars.

As mentioned above, no metals are included in our atmosphere calculations in the form of either continuum opacity or line blanketing. The latter omission may be of some concern here, in view of the rich ultraviolet metal line spectrum reported in high-dispersion *IUE* observations of several bright sdB or sdOB stars (Baschek, Kudritzki, and Scholz 1980; Baschek *et al.* 1982; Baschek, Höfflich, and Scholz 1982; Heber *et al.* 1984*a*; Lamontagne *et al.* 1985). The adequacy of atmospheric models with partial metal line blanketing has already been investigated by Heber *et al.* (1984*b*). They performed a comparison of far-ultraviolet (*IUE* only) and optical energy distribution fits obtained with both Kurucz's (1979) fully blanketed models and their own grid of models with partial metal line blanketing. Their tests suggest that the use of Kurucz's fluxes results in effective temperatures ~500 K hotter than those derived with their own set of models. Accordingly, we have used the Kurucz (1979) grid of solar abundance models at log g = 4.5 and 5.0 as our second set of model calculations. Unfortunately, the frequency grid near the Lyman edge is rather crude for our intended detailed fit to the *Voyager* data in that spectral range. A comparison of the fits obtained with Kurucz's models and our own provides, nevertheless, some insight into the adequacy of these grids and is further discussed in § IV*a*.

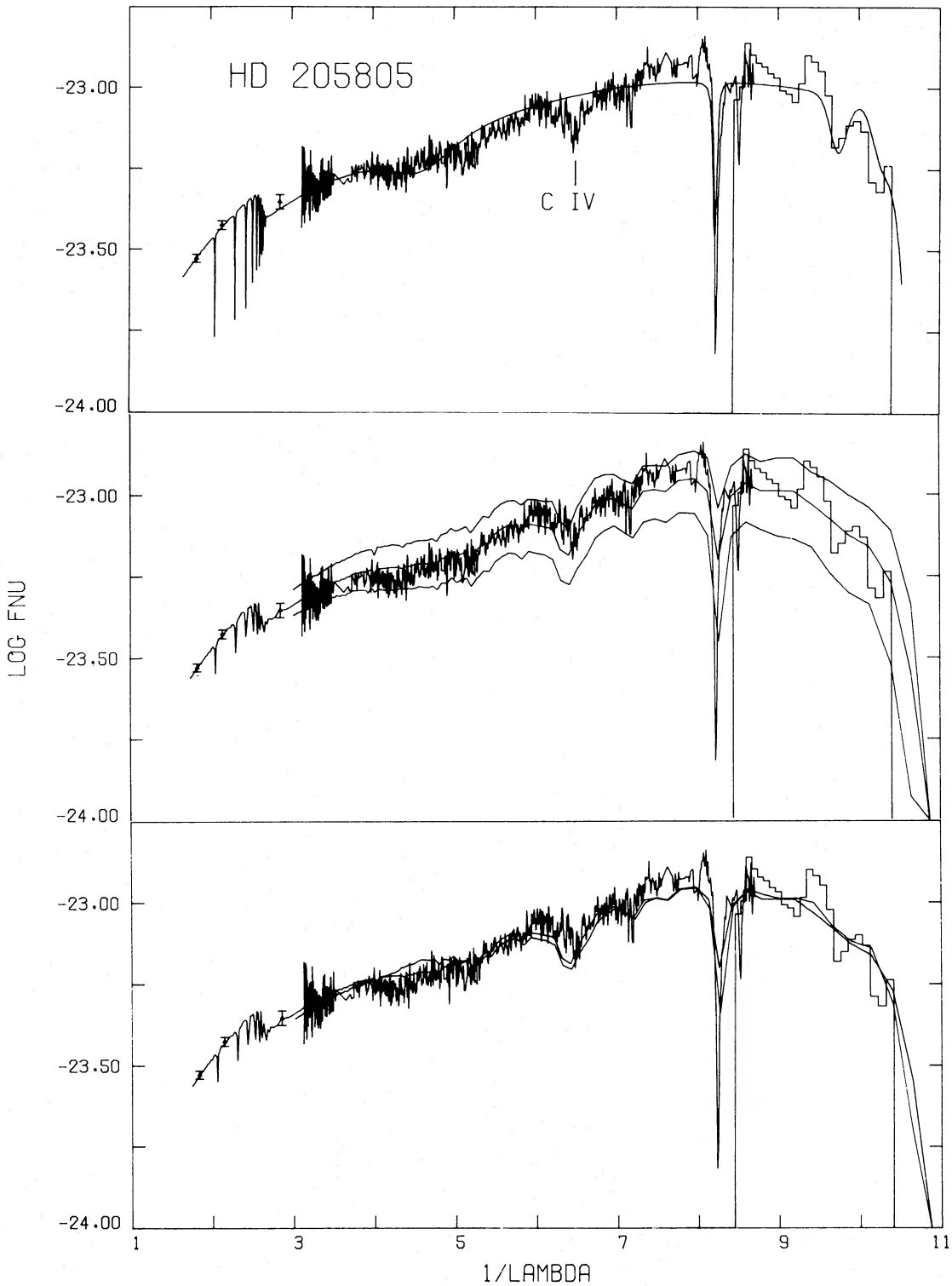

FIG. 2.—The complete energy distribution of the subdwarf B star HD 205805, together with several model atmosphere fits. The *Voyager* data are displayed as a histogram, the *IUE* data as a solid line, and the Strömgren *u*, *b*, and *y* magnitudes as three points with associated error bars. The top panel displays the optimal fit achieved with the metal-free models (T_e = 29,100 K, $E(B-V) = 0.08$); the position of the strong C IV λ1550 line, not predicted in these, is indicated. The middle panel shows the optimal fit achieved with Kurucz's (1979) solar-composition, metal-line blanketed models [T_e = 27,200 K, $E(B-V) = 0.05$], together with the fits achieved with models with identical reddening but effective temperatures that differ by $\pm$3000 K from that of the optimal fit. For clarity, only the region $1/\lambda > 3$ μm^{-1} is shown for these. The bottom panel shows a comparison of the optimal fits obtained with Kurucz's models with the color excess free to vary [T_e = 27,200 K, $E(B-V) = 0.05$, as in the middle panel], and with $E(B-V) \equiv 0$ (T_e = 24,200 K). The model with a color excess provides a marginally better fit in the region around $1/\lambda$ = 4–5 μm^{-1}.

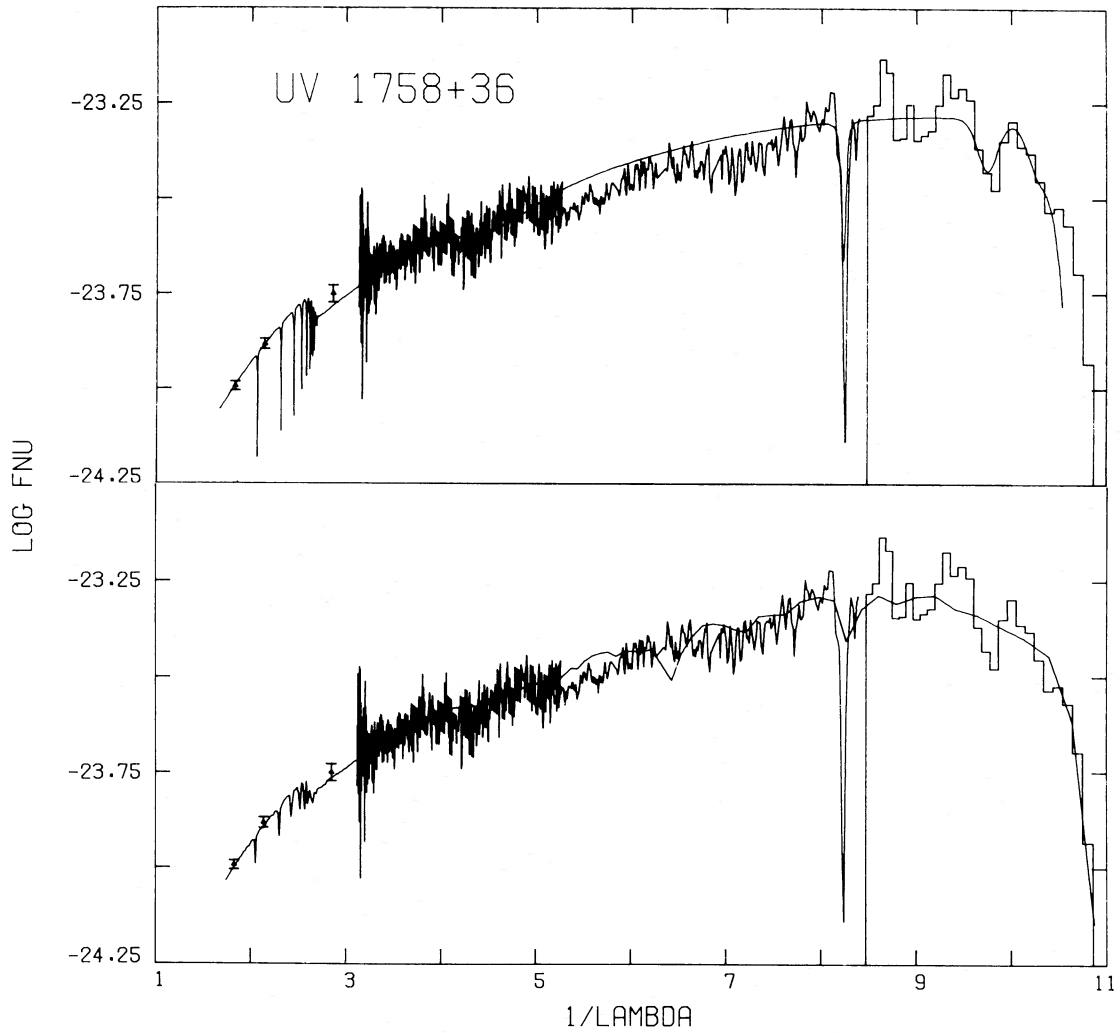

FIG. 3.—Same as Fig. 2, for UV 1758+36. The top panel displays the fit achieved with the grid of metal-free models [T_e = 31,000 K, $E(B-V) = 0.04$]; the bottom panel displays that obtained with Kurucz's (1979) solar-composition, metal-line blanketed models [T_e = 32,500 K, $E(B-V) = 0.04$]. The latter set provides a better fit to the region covered by the SWP camera (5 $\mu m^{-1} \leq 1/\lambda \leq 8$ μm^{-1}).

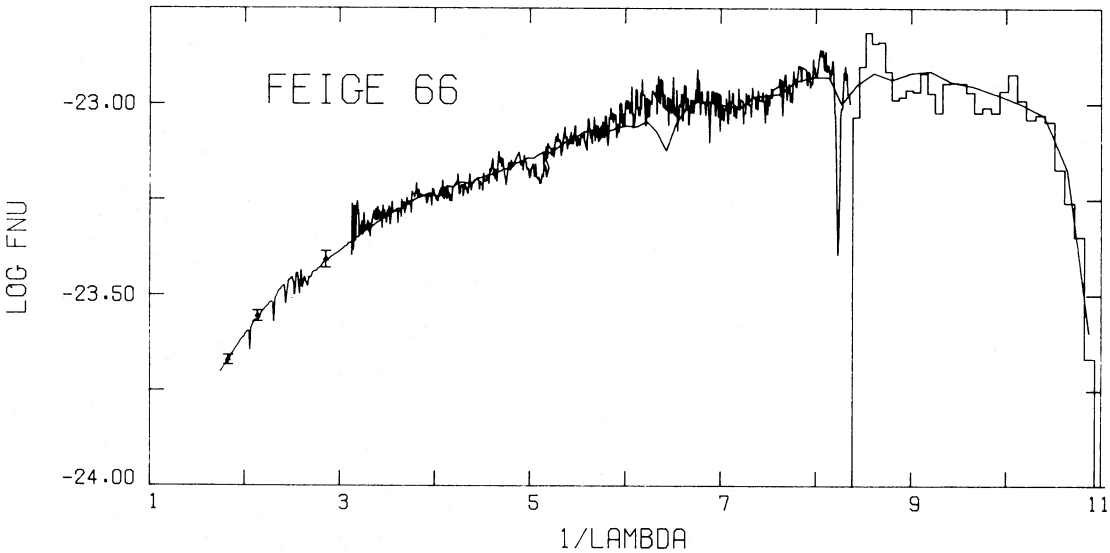

FIG. 4.—Same as Fig. 2, for Feige 66. The fit displayed is that achieved with Kurucz's (1979) solar-composition, metal-line blanketed models [T_e = 35,700 K, $E(B-V) = 0.04$].

b) *Method of Analysis*

The effective temperature of our target stars was obtained by performing a least-squares fit to the complete energy distribution over the range 950–5500 Å. For this purpose, the theoretical fluxes from our metal-free models were first folded with a Gaussian to mimic the instrumental resolution of both the *IUE* and the *Voyager* detectors. The adopted FWHM were 25 Å for $\lambda \leq 1175$ Å, and 7 Å for 1175 Å $\leq \lambda \leq 1400$ Å. For Kurucz's (1979) models, no such convolution was performed because of the sparser frequency grid available. Both the theoretical and observed fluxes in the *IUE* range were then averaged over 40 Å bins. The theoretical fluxes in the *Voyager* range were simply sampled over intervals of 9.26 Å, to match the spectrometer channel width.

Our numerical procedure consists of a three-dimensional least-squares fit to the energy distribution, as the effective temperature, the solid angle, and the amount of interstellar reddening along the line of sight need to be determined. Because of the small gravity sensitivity of the energy distribution, no attempt is made here to determine log g; rather, the data are analyzed in terms of model grids of fixed surface gravity. The interstellar extinction is taken into account as described below (§ IIIc). For each combination of effective temperature and color excess, the optimal solid angle is first determined by minimizing the residuals of the energy distribution fit *over the complete wavelength baseline.* A two-dimensional table of minimum residuals (and associated solid angles) can then be generated. The optimal values of T_e and $E(B-V)$ are then determined through a search for a true minimum in the two-dimensional array.

c) *The Treatment of Interstellar Reddening*

In energy distribution fits based on optical and *IUE* spectrophotometry of hot, lightly reddened stars, it is often possible to obtain fits of comparable quality either with unreddened model fluxes or with somewhat hotter models with a small amount of extinction. This nagging uncertainty is of some concern even when the wavelength baseline of the observations is extended below ~1200 Å. In that region, the observed fluxes are sensitive to both the ultraviolet extinction, which rises steeply below Lyα, and to the effective temperature. Accordingly, we decided to include the effects of interstellar reddening self-consistently in our analysis, even though, at the Galactic latitude of our three program objects ($b = -47°.8$, $+25°.4$, and $+86°.2$ for HD 205805, UV 1758+36, and Feige 66 respectively), only small amounts of interstellar extinction are expected. In that respect, our method differs from that of Heber *et al.* (1984*b*), where the effective temperature is first obtained from unreddened energy distribution fits, and the reddening then determined solely from the optical colors.

All theoretical spectra used in the fits were reddened with the use of Seaton's (1979) mean ultraviolet extinction curve. For our purpose, that fit—which is given as valid out to $1/\lambda = 10\ \mu m^{-1}$—was extrapolated out to the Lyman edge ($1/\lambda = 10.98\ \mu m^{-1}$). At that location, we find $A_\lambda/E(B-V) = 16.89$; this is about 0.85 mag less extinction (per unit color excess) than in the extrapolation of Drilling, Holberg, and Schönberner (1984) based on a different ultraviolet extinction curve. The effect of this extinction on the ultraviolet fluxes is to depress the far-ultraviolet continuum ($\lambda < 1800$ Å) and to produce an absorption trough at 2200 Å. The recent study by Greenberg and Chlewicki (1983) discusses the relevance of such an average extinction curve and shows that, as was anticipated in earlier studies, only a poor correlation is found between the far-ultraviolet extinction and the 2200 Å hump in their sample of reddened early-type stars. An equally poor correlation is found between the far-ultraviolet and optical extinctions.

In the present analysis, it was found that some, albeit small, ultraviolet extinction was indeed required to fit all three stars, in the sense that the optimal theoretical model with extinction included usually led to smaller postfit residuals than its counterpart without extinction. In the reddened models, the influence of the ultraviolet extinction over the range 950–1800 Å is weighted more heavily than the appearance of the 2200 Å hump, as the former is spread over more wavelength bins. Thus, the value of $E(B-V)$ adopted in the optimal model is primarily a measure of the extinction below 1800 Å, and less of the strength of the 2200 Å hump or of the optical extinction.

IV. RESULTS

a) *Effective Temperature Determinations*

Our optimal temperature fits are presented in Figures 2, 3, and 4. For the classical sdB star HD 205805, the best fit obtained with our grid of metal-free energy distributions yields $T_e = 29{,}100$ K, $E(B-V) = 0.08$. That fit is displayed in the top panel of Figure 2. The color excess required to fit the far-ultraviolet energy distribution shortward of ~1800 Å produces a shallow 2200 Å hump, not incompatible with the *IUE* long-wavelength camera data. The central depth of Lyβ is reproduced satisfactorily, but the fit in the far wings of Lyα is less satisfying. The *Voyager* flux uncertainty is in the 15%–25% range longward of 9 μm^{-1} but drops below ~10% shortward of 1075 Å; nevertheless, our fit to the red wing of Lyβ still appears too crude. The metal-free models reproduce neither the strong C IV feature seen in the low-dispersion *IUE* image nor the details of the complex *IUE* energy distribution, which are most likely due to metal line blanketing. Accordingly, we have also analyzed the data on HD 205805 with the Kurucz (1979) models. The resulting optimal fit yields $T_e = 27{,}200$ K, $E(B-V) = 0.05$ (Fig. 2, *middle panel*). While the quality of the fit in the SWP range has obviously improved with the solar-composition models, the fit below 1100 Å is less satisfactory, due primarily to the coarseness of the frequency grid in that region. Also displayed in that panel are model fits with effective temperatures differing from the optimal value by ±3000 K (and with the same color excess). These fits are representative of the temperature discrimination afforded by fits to the complete energy distribution. Finally, in the bottom panel of Figure 2, we compare the fits obtained with and without interstellar reddening taken into account. The reddened and unreddened energy distributions provide fits of comparable overall quality, with the reddened fluxes providing, nevertheless, a marginally better match to the LWR data and smaller residuals. The effective temperature difference between the optimal reddened and unreddened models is ~3000 K. Tests performed on our objects have shown that the inclusion of *Voyager* data in the analysis can reduce significantly the uncertainty in the effective temperature due to a small but unknown color excess by an amount ranging from ~500 K to ~4000 K. We thus adopt for HD 205805 an average effective temperature based on our reddened energy distribution fits of $T_e = 28{,}200 \pm 1300$ K. This temperature is in good agreement with that determined by Baschek and Norris (1970), based exclusively on their optical narrow-band

photometry and a reddening-free temperature sensitive index q, viz., $T_e = 26{,}500^{+1500}_{-1300}$ K.[5]

For the intermediate-temperature sdB star UV 1758+36, our fitting procedure with the metal-free models yields $T_e =$ 31,000 K, with $E(B-V) = 0.04$; this optimal fit is displayed in the top panel of Figure 3. The ultraviolet observations in the *Voyager* range are reproduced satisfactorily, but the fluxes in the range of the SWP camera fall consistently 10%–15% below those of the optimal model. An improved fit in this range is possible with Kurucz's (1979) models, and this result is shown in the bottom panel of Figure 3. The solar-composition model ($T_e = 32{,}500$ K, $E(B-V) = 0.04$) provides a better match to the *IUE* data below 2000 Å, which suggests that the overall metal line blanketing may be more severe in UV 1758+36 than in HD 205805; however, the solar carbon abundance in the model appears too high for the former, a result substantiated by the abundance analysis of Lamontagne *et al.* (1985). Once again, the Kurucz (1979) models reproduce only the crudest features of the energy distribution below 1100 Å. For UV 1758+36, our adopted final temperature is thus $T_e = 31{,}800 \pm 1100$ K. This final value is close to that determined by Giddings and Dworetsky (1978), $T_e = 32{,}500$ K $\pm$ 2500 K, which was based exclusively on a fit to the Hδ line profile. Furthermore, these authors also derived an approximate color excess $E(B-V) = 0.05$, which they used to deredden the S2/68 data. This value, obtained from optical color information, was shown by them to yield dereddened ultraviolet fluxes ($\lambda \geq 2000$ Å) consistent with their effective temperature determination. The S2/68 data also suggested the possiblity of some metal line blocking for $\lambda \leq 2000$ Å, a result strengthened by the *IUE* data presented here.

Our optimal fit to the Feige 66 observations, using Kurucz's (1979) models, is achieved for $T_e = 35{,}700 \pm 1500$ K and is displayed in Figure 4. The theoretical energy distribution is that of a fully blanketed model at $T_e = 35{,}700$ K, with $E(B-V) = 0.04$. An additional and interesting result of this fit is the complete failure of the metal-free models to reproduce the energy distribution of Feige 66. This is primarily due to the uneven shape of the *IUE* flux distribution between 4 and 8 μm^{-1} (see Fig. 4). To accomodate this shape with unblanketed models, our minimization procedure tends toward hot ($T_e \geq$ 45,000 K) and appreciably more reddened [$E(B-V) \geq 0.07$] theoretical energy distributions, which then fail to fit the Lyβ strength, tend to yield an unacceptably strong 2200 Å hump, and, overall, produce a poor match to the data. The blanketed models, on the other hand, fit the observed data quite well over the 4–8 μm^{-1} range (except, once again, for the strong predicted C IV feature) and also fit satisfactorily the overall continuum shape below 1200 Å. Thus, in this case at least, the strong blanketing of the numerous metal lines simply cannot be overlooked in the energy distribution fit.

b) *Uncertainties Associated with the IUE Calibration*

In order to study the importance of the time-dependent sensitivity degradation of the *IUE* cameras for the present investigation, we have performed some tests which include the correction suggested by FBB. However, a fully consistent investigation of the influence of that correction is not possible here because of the disparity in the dates of acquisition of the various *IUE* images; thus, for example, the two images of HD 205805 are so recent (1983.49) that no corrections are available, and an uncertain extrapolation outside the FBB data would be required for both cameras. In the case of UV 1758+36, the FBB correction can be applied straightforwardly to the SWP image (1980.16), while no correction is available for the more recent LWR image (1983.62). The inverse is true for Feige 66.

For hot objects, the influence of the FBB correction is larger when applied to the SWP camera instead of the longer wavelength (LWR) data. Hence, we restrict our brief discussion of the FBB correction to the fit of UV 1758+36, in which we correct the SWP but not the LWR camera data. When applied in conjunction with the fit based on the metal-free models, the FBB correction yields an optimal effective temperature ($T_e =$ 30,800 K) which differs only marginally (−200 K) from that obtained without applying the correction. For the fit with the metal-line blanketed models, the resulting effective temperature is identical to that obtained without the inclusion of the FBB correction. For both grids of models, the postfit residuals with and without the FBB factor differ by only a few percent. Clearly, the ability to complement the *IUE* energy distributions with *Voyager* data reduces considerably the margin of maneuver in the fits and permits effective temperature determinations which are less dependent on the still poorly documented degradation of the *IUE* sensitivity. This result is confirmed by further tests which leave out the *Voyager* data altogether from the fit. In that case, the optimal effective temperatures are somewhat higher than those obtained with the *Voyager* data included, and the temperature changes brought about by the FBB correction are significant; we now find temperature increases of +2000 K and +2900 K for the metal-free and Kurucz models respectively, when the FBB correction is included.[6] Hence, the inclusion of *Voyager* data in our effective temperature fits provides a welcome reduction of the uncertainty associated with the *IUE* sensitivity degradation.

V. CONCLUDING REMARKS

We have presented and discussed new far-ultraviolet spectrophotometry of three hot B/OB subdwarfs obtained with the *Voyager* spectrometers. When combined with optical photometry and with existing ultraviolet spectrophotometry from *IUE*, these observations permit virtually complete energy distributions to be constructed over the range 950–5500 Å. Model energy distributions, both with and without metal-line blanketing, have been used to determine effective temperatures for the program objects. The model atmosphere calculations generally provide satisfactory fits to the observed energy distributions. The derived effective temperatures are also in good agreement with previous determinations, which were based exclusively on optical photometric and spectroscopic information. Apart from the intrinsic interest of the far-ultraviolet spectrum of hot subdwarfs below ~1200 Å, *Voyager* observations provide two additional advantages over previous temperature determinations based on energy distribution fits:

[5] We note that the use of the Strömgren-based reddening-free index Q' ($Q' = +0.146$), instead of the Newell index q (see Baschek and Norris 1970) would yield $T_e = 28{,}000$ K, on the basis of the calibration of Bergeron *et al.* (1984).

[6] These results are in agreement with those that can be read off the FBB figures; for a 30,000 K star, the calibration of FBB—which is based on DA white dwarfs—suggests that the effective temperature based on *IUE* energy distribution fit could be *underestimated* by ~2000–3000 K if the sensitivity degradation of the *IUE* cameras is ignored.

First, they allow a determination of the interstellar reddening along the line of sight in a more self-consistent way. Second, they help reduce some of the uncertainties (modeled here according to the FBB results) associated with the *IUE* calibration. Eventually, such results should contribute to a better definition of the temperature scale for hot, hydrogen-rich subdwarfs.

We are grateful to the Astronomical Data Center at the NASA/Goddard Space Flight Center for providing us with archived *IUE* images. Our thanks are also extended to the Director of Kitt Peak National Observatory for the continuing support of our observing program, and to the staff of KPNO and *IUE* for their help with data acquisition. This work was supported in part by the NSERC Canada and by NASA grants NAGW-587 and NAG5-411. Computing funds for this project were kindly provided by the Centre de Calcul of the Université de Montréal.

REFERENCES

Baschek, B., Höfflich, P., and Scholz, M. 1982, *Astr. Ap.*, **112**, 76.
Baschek, B., Kudritzki, R. P., and Scholz, M. 1980, in *Proc. Second European IUE Conference* (ESA SP-157), p. 319.
Baschek, B., Kudritzki, R. P., Scholz, M., and Simon, K. P. 1982, *Astr. Ap.*, **108**, 387.
Baschek, B., and Norris, J. 1970, *Ap. J. Suppl.*, **19**, 327.
Berger, J. 1963, *Pub. A.S.P.*, **75**, 393.
Bergeron, P., Fontaine, G., Lacombe, P., Wesemael, F., Crawford, D. L., and Jakobsen, A. M. 1984, *A.J.*, **89**, 374.
Boksenberg, A., *et al.* 1973, *M.N.R.A.S.*, **163**, 291.
Broadfoot, A. L., *et al.* 1977, *Space Sci. Rev.*, **21**, 183.
———. *et al.* 1981, *J. Geophys. Res.*, **86**, 8259.
Drilling, J. S., Holberg, J. B., and Schönberner, D. 1984, *Ap. J.* (*Letters*), **283**, L67.
Edmonds, F. N., Jr., Schlüter, H., and Wells, D. C., III, 1967, *Mem. R.A.S.*, **71**, 271.
Finley, D. S., Basri, G., and Bowyer, S. 1984, in *Future of Ultraviolet Astronomy Based on Six Years of IUE Research*, ed. J. M. Mead, R. D. Chapman, and Y. Kondo (NASA CP-2349), p. 277 (FBB).
Fontaine, G., Wesemael, F., Lamontagne, R., Bergeron, P., and Green, R. F. 1985, in preparation.
Giddings, J. R., and Dworetsky, M. M. 1978, *M.N.R.A.S.*, **183**, 265.
Graham, J. A. 1970, *Pub. A.S.P.*, **82**, 1305.
Graham, J. A., and Slettebak, A. 1973, *A.J.*, **78**, 295.
Greenberg, J. M., and Chlewicki, G. 1983, *Ap. J.*, **272**, 563.
Greenstein, J. L., and Sargent, A. I. 1974, *Ap. J. Suppl.*, **28**, 157.
Hackney, R. L., Hackney, K. R. H., and Kondo, Y. 1982, in *Advances in Ultraviolet Astronomy: Four Years of IUE Research*, (Washington: NASA), p. 335.
Heber, U. 1985, *Astr. Ap.*, in press.
Heber, U., Hamann, W.-R., Hunger, K., Kudritzki, R. P., Simon, K. P., and Mendez, R. H. 1984*a*, *Astr. Ap.*, **136**, 331.
Heber, U., and Hunger, K. 1984, in *Proc. Fourth European IUE Conference* (ESA SP-218), p. 273.
Heber, U., Hunger, K., Jonas, G., and Kudritzki, R. P. 1984*b*, *Astr. Ap.*, **130**, 119.
Holberg, J. B., Forrester, W. T., Shemansky, D. E., and Barry, D. C. 1982, *Ap. J.*, **257**, 656.
Holberg, J. B., Sandel, B. R., Forrester, W. T., Broadfoot, A. L., Shipman, H. L., and Barry, D. C. 1980, *Ap. J.* (*Letters*), **242**, L119.
Holberg, J. B., Wesemael, F., and Hubený, I. 1984, *Ap. J.*, **280**, 679.
Holberg, J. B., Wesemael, F., Wegner, G., and Bruhweiler, F. C. 1985, *Ap. J.*, **293**, 294.
Kurucz, R. L. 1979, *Ap. J. Suppl.*, **40**, 1.
Lamontagne, R., Wesemael, F., Fontaine, G., and Sion, E. M. 1985, *Ap. J.*, **299**, in press.
Newell, E. B., and Graham, J. A. 1976, *Ap. J.*, **204**, 804.
Sargent, W. L. W., and Searle, L. 1968, *Ap. J.*, **152**, 443.
Seaton, M. J. 1979, *M.N.R.A.S.*, **187**, 73P.
Vidal, C. R., Cooper, J., and Smith, E. W. 1973, *Ap. J. Suppl.*, **25**, 37.
Wesemael, F., Auer, L. H., Van Horn, H. M., and Savedoff, M. P. 1980, *Ap. J. Suppl.*, **43**, 159.

G. FONTAINE, R. LAMONTAGNE, and F. WESEMAEL: Département de Physique, Université de Montréal, C. P. 6128, Succ. A, Montréal, Québec H3C 3J7, Canada

J. B. HOLBERG: Lunar and Planetary Laboratory, University of Arizona, 3625 East Ajo Way, Tucson, AZ 85713

S. VEILLEUX: Department of Astronomy, University of California, Santa Cruz, CA 95064